metals

Article

The Challenge of Impurities (Fe, Si) to Recycling in the Rolled Aluminum Industry in the Coming Years in Relation to Their Influence on Ultimate Tensile Strength

Mateo M. Vicent Fanconi [1,2], Ignacio Gil Fernández-Marcote [1] and Íñigo Ruiz-Bustinza [2,*]

[1] Cindal R&D, Aludium Transformación de Productos S.L.U., 03008 Alicante, Spain; mateo.vicent.fanconi@alumnos.upm.es (M.M.V.F.); ignacio.gilfernandez-marcote@aludium.com (I.G.F.-M.)

[2] Departamento de Ingeniería Geológica y Minera, Escuela Técnica Superior de Ingenieros de Minas y Energía, Universidad Politécnica de Madrid, 28040 Madrid, Spain

* Correspondence: inigo.rbustinza@upm.es; Tel.: +34-910676547

Abstract: The increased recycling in aluminum production has raised the impurity content in the industry, thus increasing its effect on mechanical characteristics and making it difficult for recycled products to meet the properties' goals as their effect is not yet sufficiently known. Therefore, the two main impurities (Fe and Si) in standard aluminum rolling mill products of alloy 5754 were investigated to determine their effects on the ultimate tensile strength (UTS). After analyzing the composition, mechanical properties, and microstructure, the relationship of both impurities with the UTS in fully annealed products was estimated by statistical analysis, obtaining a strong influence of Si and Fe.

Keywords: aluminum; scrap; ultimate tensile strength; impurities; recycling

check for updates

Citation: Vicent Fanconi, M.M.; Gil Fernández-Marcote, I.; Ruiz-Bustinza, Í. The Challenge of Impurities (Fe, Si) to Recycling in the Rolled Aluminum Industry in the Coming Years in Relation to Their Influence on Ultimate Tensile Strength. *Metals* **2023**, *13*, 2014. https://doi.org/10.3390/met13122014

Academic Editor: Mohammad Jahazi

Received: 6 November 2023
Revised: 30 November 2023
Accepted: 4 December 2023
Published: 15 December 2023

1. Introduction

The market forecasts a continuous growth of aluminum alloy demand until at least 2050 [1,2]. This, based on the thesis of facing finite resources and environmental sustainability issues, involves an important risk: the need to resort to recycling, as already pointed out in the UN Sustainable Development Goals in Goal 12 "Responsible Consumption and Production", aiming at a circular economy with ideally 100% recycling [3].

This, combined with government policies and the economic advantage of recycling, has led the aluminum industry to increase its recycling rate to 50–90%, depending on the company, region, and product [4–10].

Aluminum production is classified by manufacturing methods into wrought and cast products, which are divided into alloys, and these are grouped into series depending on which is the main alloying element.

The wrought alloys are grouped into the following series: 1xxx: purity (<1% by mass of other elements); 2xxx: copper; 3xxx: manganese; 4xxx: silicon; 5xxx: magnesium; 6xxx: silicon and magnesium; 7xxx: zinc; and 8xxx: others. In the cast production, Si is the main alloying element [11].

This series scenario is important to understand the actual impurities contribution since, within the aluminum scrap with such typical alloys and considering that the industry is currently far from segregating the scrap with perfect efficiency, a significant amount of the impurities will be due to these five alloying elements (in addition to the contaminations and initial impurities, mainly Fe) [9–12].

Hence, these impurities are irreversibly incorporated into the product once it is melted because currently, there are no industrially and economically viable methods for purifying low-purity aluminum [9,10,13–15].

The impurity content of products will increase as recycling cycles continue, and the impurity content of scrap will not consequently decrease. This, combined with the increasing interest in recycling, will result in products being loaded with impurities up to the maximum allowable limit. This occurs, for instance, in the 5xxx series alloys with Si, which is a key impurity in this series.

The scrap used by the foundries for the production of the 5xxx series alloys, in addition to the internal or process scrap at each plant (which will correspond to the same alloy), shall come mainly from the 6xxx series alloys [16] with a Si content close to 0.6%w/w [11] or higher in case of contamination with casting alloys, which are increasingly available in the scrap market and for whose products there is less demand, thus reducing the amount of scrap contaminated with high Si contents that can be diverted for their production. [1,9,16] This means that the Si content in the alloys of this series is increasing.

A study was carried out with the company Aludium regarding Si content levels in the 5754 alloy, of which a significant amount is currently produced (more than 50,000 tons per year) Figure 1.

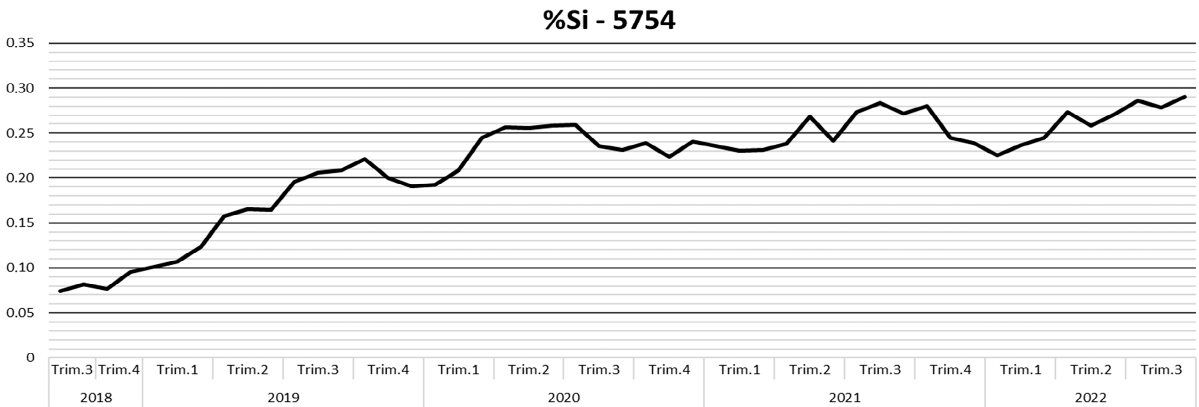

Figure 1. Percentage of silicon (%w/w) in Aludium's 5754 products.

As seen in the graph, the Si content in 5754 products tripled from 0.1% to 0.3% from the third quarter of 2018 to the third quarter of 2022, with a maximum limit of 0.40% according to EN573-3 [17]. Specifically, most of the increase occurred between the fourth quarter of 2018 and the second quarter of 2020, coinciding with an increase in the percentage of external scrap in the melt mix to produce this alloy (from approximately 10% to 50%).

This increase is explained by the increased use of external scrap or the switch to external scrap more contaminated in Si, so that with each production cycle the internal scrap becomes more contaminated, increasing the Si content in the final product up to a maximum level, which can be approximated by Equation (1) (the Si contribution of primary aluminum is neglected).

$$\%Si \approx \frac{External\ Scrap\ \%Si\ * \%\ External\ Scrap}{1 - \%\ Internal\ Scrap} \tag{1}$$

Since the amount of internal scrap is not easily variable because it depends on productivity, and returns to low Si values it would be necessary to use cleaner external scrap, with the consequent economic cost, or to reduce the use of scrap, with the consequent economic and environmental cost.

Because of these costs, these high levels of Si will likely continue to be tolerated until a purification system can be implemented.

Another problem is that with the higher use of external scrap, the content of Si will eventually exceed the allowed limit by the EN standard in the alloy. This could be solved by changing the silicon limits in the standard to accommodate current recycling requirements, although a higher percentage of Si may create other problems [18–20].

This example is not far from the situation in many other high-capacity recycling facilities and can be extended to other impurities and alloys [1,11,16,21], such as Fe in the same aluminum alloy (Figure 2). Not only will impurity levels be a major limiting factor in recycling until purification systems are implemented, but they will also pass from negligible percentages to alloy-like concentrations.

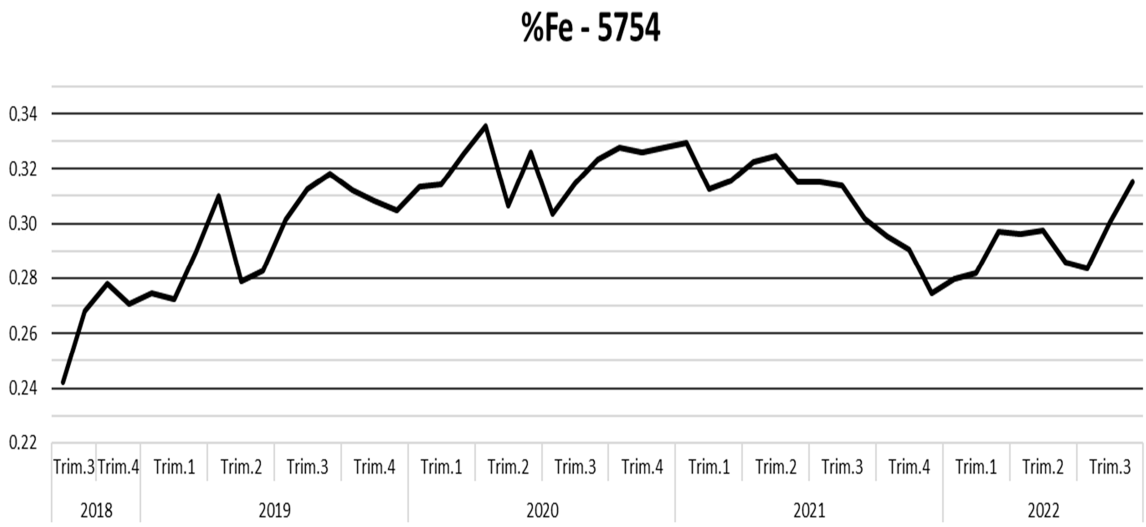

Figure 2. Percentage of Fe (%w/w) in Aludium's 5754 products.

In the past, detailed studies [18,20] explaining the effects of chemical constituents on the properties of an aluminum alloy were limited to the alloying elements themselves, while the effect of impurities on many properties (especially mechanical properties) was less evaluated due to their very low content [22]. However, as shown above, this is no longer the case, so the study of their effects on the properties of the final product is of great interest, as recent publications have shown [9].

Since the Si and Fe contents in alloy 5754 will remain high in the near future, their effect on the ultimate tensile strength (UTS) was studied. The current literature teaches that constituents (alloying elements or impurities) tend to strengthen the metal, either in solid solution, by hindering the movement of atoms, or by forming precipitates that anchor the grains and thus hinder the deformation [23].

It is known that Fe refines the grain by precipitating particles that stimulate nucleation (particle-stimulated nucleation [24]), thereby increasing the UTS in what is known as the grain refinement hardening effect or the Hall–Petch effect [25]. This mechanism is exploited in the 8xxx series where Fe is alloyed, such as in alloys 8005, 8006, and 8011 [19,23,26].

Si, like all the constituents, strengthens the alloy and produces particles that increase the UTS, as is the case in the 4xxx series. In the 6xxx series, the Si combined with the Mg increases the UTS through a heat treatment that exploits the precipitation of magnesium silicides (Mg_2Si) [27,28].

Therefore, in alloy 5754, it was expected that both impurities (Fe and Si) would increase the UTS. To verify this, this study was carried out, which also seeks to quantify the effect of these impurities on the ultimate tensile strength [9,19].

2. Materials and Methods

The composition and mechanical property data of alloy 5754 products of Aludium were studied to determine the effect of these impurities on the ultimate tensile strength (UTS). The composition was determined with an optical emission spectrometer (Quantometer) model ARL 3460 and 3560 (ThermoFisher SARL, Ecublens, Switzerland) from samples taken from the liquid metal (molten aluminum) with a horizontal disk tester. The UTS was measured on an Instron 5985 universal testing machine (Instron GmbH, Darmstadt, Germany) using an ISO 6892-1 test [29].

A rolled product not submitted to cold rolling was selected from the production of 5754 of Aludium for this study. Thus, it is a product in the total annealing condition, which is the one with the lowest UTS due to the heat treatment, namely, the Product A sample [30].

Statistical samples were generated from Product A data in which the contents of Si, Fe, and Mg (the major alloying element of 5754) varied while the contents of the other elements were fixed or within a narrow range. Pearson's correlation coefficient was used to determine the relationship between the Si, Fe, and Mg contents and UTS. The structure, matrix, and constituent contents of five samples of Product A with similar Mg contents but different Si contents were analyzed by field emission scanning electron microscopy using a Thermofisher FESEM model APREO 2 scanning electron microscope (Thermofisher SARL, Ecublens, Switzerland).

To quantify the effect of impurity content on UTS, a multiple linear regression (Equation (2)) was performed selecting the contents of Si, Fe, and Mg (single or combined) as independent variables (matrix $[X]$) and the UTS values $[Y]$ as dependent variables, obtaining the factors that multiply the content of each element to estimate the UTS $[F]$. This regression assumes that the UTS does not depend entirely on the dependent variables (0%w/w of Si, Fe, and Mg does not mean zero UTS).

$$[F] = \left([X]^t * [X]\right)^{-1} * [X]^t * [Y] \quad (2)$$

To compare the influence of impurities on the UTS of cold-reduced products, a product with the same alloy as Product A and under the same conditions but with a higher cold reduction before total annealing, was analyzed and identified as Product B. Its data were also statistically analyzed.

All the material analyzed comes from industrial production with an inherent variability much greater than that of a laboratory, therefore a greater relevance will be given to the correlations found than would be the case in a study confined to a laboratory.

3. Results and Discussion

In the Product A sample, the correlation (R) between Fe and the ultimate tensile strength (UTS) is very low (R = 0.03), but there appears to be a certain negative relationship between the Si content and UTS (R = −0.38). (The latter seems to contradict the strengthening effect of Si expected from the literature.

To understand the hardening mechanism of Mg, is necessary to explain this negative correlation between the Si content and the UTS. The main alloying element in a 5xxx series alloy, Mg, is the most hardening element due to the distortion in the aluminum atomic lattice produced when in solid solution [18,19,23,26,31,32]. A strong correlation (R = 0.77) is obtained between the Mg content and the UTS of the selected sample. It is known that Si in the presence of Mg precipitates as Mg_2Si, which is in fact the hardening mechanism of the 6xxx series [27,33]. The hypothesis would be that the softening effect found in Si comes from its combination with Mg atoms, taking it out from solid solution to precipitate Mg_2Si constituents, which no longer exerts a hardening effect on the lattice. Therefore, Si inhibits the hardening effect of Mg in 5754 (and all 5xxx series).

The reason for these Mg_2Si precipitates not increasing the UTS, as in the 6xxx, is that they have not been heat treated to achieve a fine and homogeneously dispersed precipitate, but they have cooled slowly down in the Mg_2Si precipitation zone, producing large particles that do not have the hardening mechanisms that occurred in the 6xxx series [18,23,27].

Five test pieces of Product A with different Si contents but similar Mg levels were selected to support this hypothesis, with the following results (Table 1). In addition, the precipitates present were analyzed to verify where the Mg deficit was located in the solid solution.

Table 1. Si and Mg composition (%*w*/*w*) of the specimens.

Specimen	Si (%wg)	Mg (%wg)
1	0.13	2.89
2	0.22	2.89
3	0.26	2.84
4	0.32	2.90
5	0.33	2.86

First, it can be observed that a higher Si content leads to a higher precipitation of Mg_2Si (Figure 3), which is the constituent with the vast majority of Mg from the solid solution (Table 2).

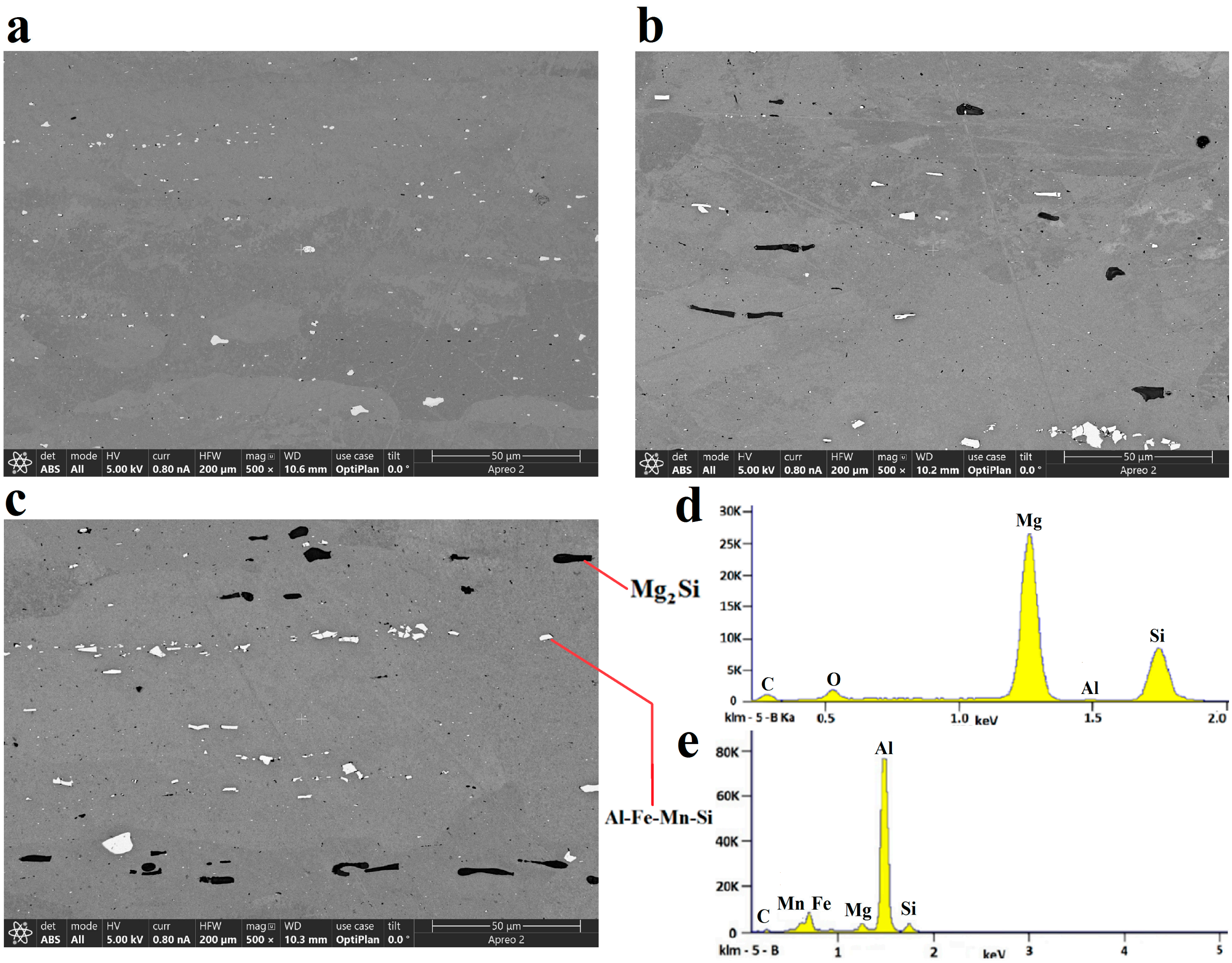

Figure 3. FESEM micrograph with backscattered electron detector (ABS), from left to right, top to bottom (**a**) Specimen 1, (**b**) Specimen 2, (**c**) Specimen 5, (**d**) EDX microanalysis of a Mg_2Si and (**e**) a constituent (Al-Fe-Mn-Si) (down) from the Specimen 5.

Table 2. Composition of the analyzed precipitates (carbon and oxygen measurements have been disregarded).

%*w*/*w*	Si	Fe	Mn	Mg	Al
Mg_2Si	37.62	-	-	62.08	0.29
Al-Fe-Mn-Si	3.05	27.99	7.45	1.70	59.82

The solid solution composition of each specimen was analyzed using SEM-EDX equipment (Thermofisher SARL, Ecublens, Switzerland) to determine the Mg content, Table 3.

Table 3. Mg in solid solution of each specimen (semi-quantitative data).

Specimen	Average Mg in Solid Solution (%*w*/*w*)
1	2.79
2	2.58
3	2.59
4	2.51
5	2.36

From these semiquantitative data and the Si and Mg contents of each sample (Table 1), the graph in Figure 4 shows how precipitated Mg (difference between %Total Mg and %Mg in solid solution) increases with increasing Si content.

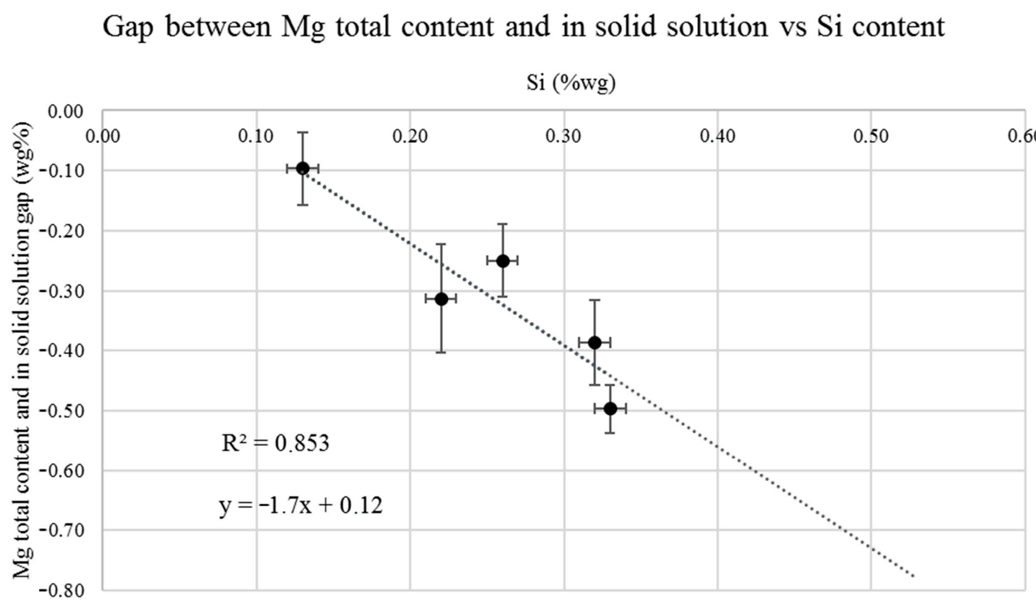

Figure 4. Relationship between the Si content and the difference between total Mg and the one present in solid solution.

The slope of the equation (Figure 4) approximating the points obtained (−1.7) is close to the one that would determine the stoichiometric ratio of the Mg_2Si precipitation reaction (Equation (3)), using the atomic weights of both elements (Si = 28.09 g/mol, Mg = 24.31 g/mol). [34]

$$2\,Mg + 1\,Si = 1\,Mg_2Si - \frac{1\,Si\ unit\ of\ mass}{28.09\ \mathrm{g{\cdot}mol^{-1}}} \cdot 2 \cdot 24.31\ \mathrm{g{\cdot}mol^{-1}} = -1.73\ Mg\ units\ of\ mass \quad (3)$$

Next, a subsample from the data of Product A in which only Si and Mg contents vary, while the other elements are kept at fixed values (or narrow ranges) was selected. A multiple linear regression was performed on this sample with the Si and Mg contents as the independent variables and the UTS values as the dependent variable (Equation (2)), obtaining Equation (4).

$$UTS\ (MPA)\ \approx 127 - 34 * (\%SI) + 31 * (\%Mg) \quad (4)$$

The results obtained by estimating the UTS with Equation (4) and the real data are relatively well correlated (R^2 = 0.740), with an average estimation error of 1.6 MPa (Figure 5). This error can be easily explained by other hardening factors, such as variations in the process or deviations from the mean obtained in the mechanical properties tests.

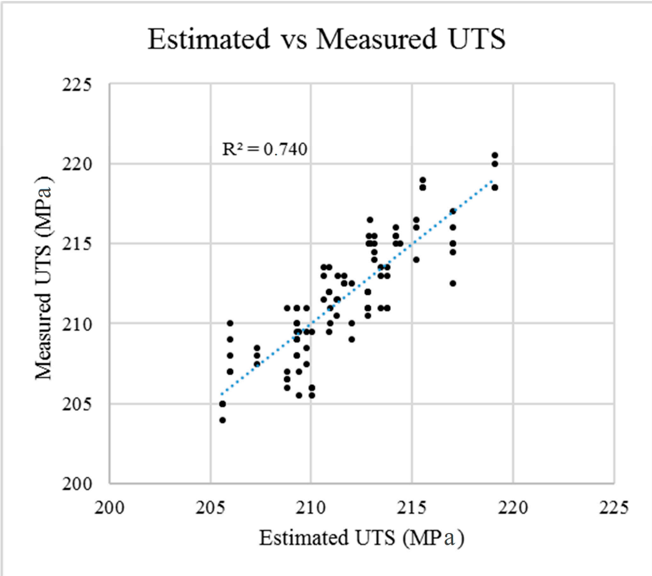

Figure 5. Estimated vs. measured UTS, Equation (4).

Other studies have already studied in detail the hardening effect of Mg, which indicates a hardening effect close to 27 MPa per weight unit of Mg content in the total annealing condition, a value close to 31 MPa of Equation (4) [31]. The softening effect of Si is equal to the effect of Mg multiplied by −1.1, thus not coinciding with the stoichiometric ratio of Mg_2Si precipitation (−1.7), although this deviation may be due to various factors such as collinearities with other elements that could not be avoided. Thus, the data used show that Si has a negative effect on the UTS of this 5754 product, although it is not possible to determine the magnitude of this effect without a more detailed study.

The formula obtained is applied to a new subsample in which the Fe content value is not fixed, resulting in a lower fit (Figure 6) and a slightly higher mean error: 1.6 MPa.

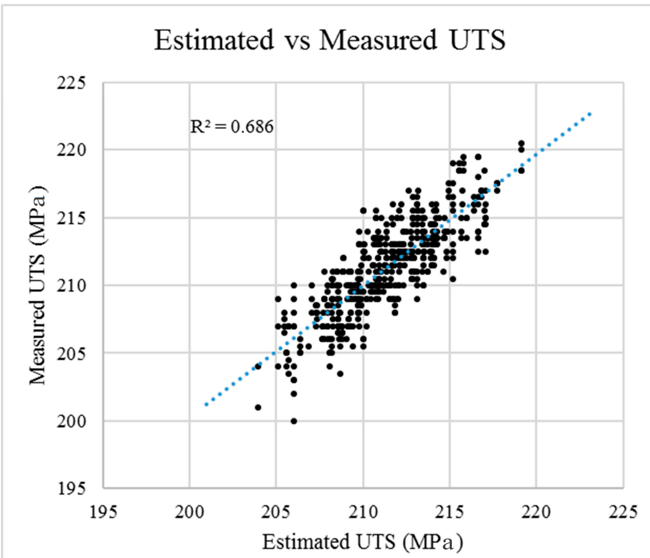

Figure 6. Measured vs. estimated UTS, Equation (4), including data with different values of Fe.

Having established that the effect of Si and Mg follows Equation (4), where one of the dependent variables is the result of the application of this equation and the other is the Fe content, another regression was performed, obtaining a new approach (Equation (5)) with the adjustment shown in Figure 7 and an average error of 1.5 MPa.

$$Rm(MPA) = 126 - 34 * (\%Si) + 31 * (\%Mg) + 9 * (\%Fe) \quad (5)$$

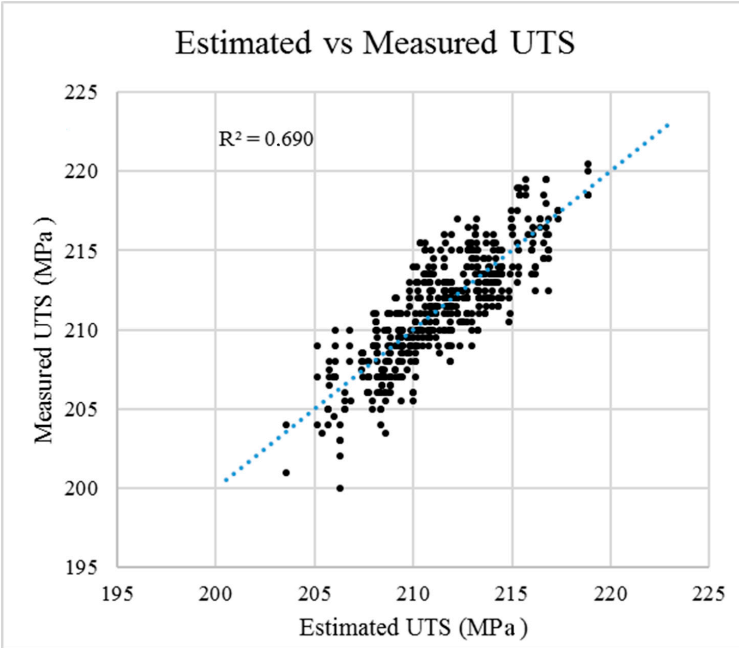

Figure 7. Measured vs. estimated UTS, Equation (5).

Although the R^2 coefficient in Figure 7 is higher, the improvement is negligible. This can be due to the small amount of Fe (Equation (6)) and therefore does not significantly correct the estimation, which would also explain the low correlation found between Fe content and UTS in Product A.

This small effect of Fe, which can be quantified as 9 MPa per 1% Fe, does not seem to agree with the 40 MPa per weight unit of Fe in the total annealed condition found in other studies [9,35]. However, when other products that have a higher cold reduction (Product A has no cold reduction) are analyzed, a greater relevance of the effect of Fe on the UTS is observed. Therefore, a product with the same alloy as Product A and under the same conditions but with a higher cold reduction before total annealing was studied, previously indicated as Product B.

In the composition and UTS data of Product B, a correlation of the latter with Si (−0.36) and Mg (0.71) as in Product A was found, but with the Fe being much higher (0.21). By multiple linear regression an estimation of the UTS (Equation (6)) with slightly higher values of the effects of Mg and Si concerning those of Product A, but with a much greater effect of Fe (9 << 32) was obtained.

$$UTS(MPA) = 103 - 48 * (\%Si) + 42 * (\%Mg) + 32 * (\%Fe) \quad (6)$$

This increase could be due, in the case of Mg, to a greater distortion of the lattice by the Mg atoms in solid solution during cold rolling, which is not recovered by the final annealing, a phenomenon known as the relationship between the work hardening coefficient and the Mg content [9,36]. This explains why, to the extent that Si inhibits the effect of the former, the ratio between the two effects in Product B concerning that of Product A is maintained (−1.1).

The increase in Fe hardening is consistent with the theory that particles stimulate nucleation during recrystallization to produce finer grains (particle-stimulated nucleation). This nucleation is facilitated by dislocations present in the lattice prior to recrystallization [24]. This, as mentioned above, increases the UTS due to the grain refinement hardening effect or Hall–Petch effect [25]. Since there is a greater cold reduction prior to recrystallization in Product B, there will be a greater number of dislocations in the lattice and the Fe constituents will be able to stimulate a higher degree of nucleation, therefore achieving a larger particle refinement and higher UTS in Product B. This explanation coincides with the negative effect of Fe on the UTS found in castings where no lamination occurs and therefore particle-stimulated nucleation cannot occur. Analysis with transmission electron microscopy could help to confirm this mechanism in future research [18,20,21].

4. Conclusions

In this study, the growth of Si and Fe contents in alloy 5754 was observed, and their limiting character in the design of casting recipes with the available raw materials. In addition, statistical analysis of the production of the company Aludium revealed the negative effect of Si on the ultimate tensile strength (UTS) in the total annealed products by causing a deficit of Mg in solid solution by precipitation of Mg_2Si, an effect that increases in products with greater cold reduction prior to the final annealing. This increase is greatest in the hardening effect of Fe, which has been found to be highly dependent on the level of cold reduction performed prior to total annealing.

This discovery has allowed the development of three equations that estimate the UTS of total annealed rolled products of alloy 5754 with less than 2% mean error. This will help to optimize the compositional design of new recycle-based products and to improve what has been recently named the science of dirty alloys [9].

Future research will illustrate the effect of all constituents on the ultimate tensile strength, yield strength, and elongation by including other alloys and extending to other tempers so that the interaction between the different stages of the manufacturing process and the effect of each constituent of the alloy on its mechanical properties can be observed. In this way, it will be possible to identify the drawbacks and advantages of this new composition scenario to design measures able to mitigate the former and enhance the latter.

Author Contributions: Conceptualization, M.M.V.F., I.G.F.-M. and Í.R.-B.; methodology, M.M.V.F. and I.G.F.-M.; software, M.M.V.F.; validation, M.M.V.F., I.G.F.-M. and Í.R.-B.; formal analysis, M.M.V.F.; investigation, M.M.V.F. and I.G.F.-M.; resources, I.G.F.-M.; data curation, M.M.V.F.; writing—original draft preparation, M.M.V.F.; writing—review and editing, Í.R.-B. and M.M.V.F.; visualization, M.M.V.F., I.G.F.-M. and Í.R.-B.; supervision, I.G.F.-M. and Í.R.-B.; project administration, M.M.V.F. All authors have read and agreed to the published version of the manuscript.

Funding: This research received no external funding.

Data Availability Statement: The data presented in this study are available on request from the corresponding author. The full data used in this study are not publicly available due to industrial privacy.

Acknowledgments: The authors acknowledge the contributions of Aludium's R&D Department and especially David Bravo Espinosa, for their help in data collection and for valuable discussions.

Conflicts of Interest: Author M.M.V.F. and author I.G.F.-M. were employed by the company Aludium Transformación de productos S.L.U. The remaining authors declare that the research was conducted in the absence of any commercial or financial relationships that could be construed as a potential conflict of interest.

References

1. Modaresi, R.; Løvik, A.; Müller, D. Component- and Alloy-Specific Modeling for Evaluating Aluminum Recycling Strategies for Vehicles. *JOM* **2014**, *66*, 2262–2271. [CrossRef]
2. Li, S.; Zhang, T.; Niu, L.; Yue, Q. Analysis of the development scenarios and greenhouse gas (GHG) emissions in China's aluminum industry till 2030. *J. Clean. Prod.* **2021**, *290*, 125859. [CrossRef]

3. United Nations—Department of Economic and Social Affairs. *The Sustainable Development Goals: Report 2022*; United Nations: New York, NY, USA, 2022.
4. Dai, M.; Wang, P.; Chen, W.; Liu, G. Scenario analysis of China's aluminum cycle reveals the coming scrap age and the end of primary aluminum boom. *J. Clean. Prod.* **2019**, *226*, 793–804. [CrossRef]
5. Norsk Hydro Asa. *Annual Report 2021*; Norsk Hydro Asa: Oslo, Norway, 2021.
6. Constellium Website. Available online: https://www.constellium.com/sustainability/promoting-recycling (accessed on 27 January 2023).
7. Novelis. *2022 Global Sustainability Report*; Novelis: Atlanta, GA, USA, 2022.
8. Aluminium Insider. Russia's Rusal Reveals Radical Refuse Recycling Regime. *Aluminium Insider*, 8 June 2022. Available online: https://aluminiuminsider.com/russias-rusal-reveals-radical-refuse-recycling-regime/ (accessed on 7 February 2023).
9. Raabe, D.; Ponge, D.; Uggowitzer, P.; Roscher, M.; Paolantonio, M.; Liu, C.; Antrekowitsch, H.; Kozeschnik, E.; Seidmann, D.; Gault, B.; et al. Making sustainable aluminum by recycling scrap: The science of dirty alloys. *Prog. Mater. Sci.* **2022**, *128*, 100947. [CrossRef]
10. Capuzzi, S.; Timelli, G. Preparation and Melting of Scrap in Aluminum Recycling: A Review. *Metals* **2018**, *8*, 249. [CrossRef]
11. *UNE-EN 13920:2003*; Aluminio y Aleaciones de Aluminio. Chatarra. AENOR: Madrid, Spain, 2003. Available online: https://www.une.org/encuentra-tu-norma/busca-tu-norma/norma/?c=N0030122 (accessed on 30 January 2023).
12. ASERAL. ASERAL—GUÍA PARA LA CLASIFICACIÓN DE CHATARRAS. Available online: http://www.aseral.es/principal.htm (accessed on 25 January 2023).
13. DeYoung, D.H.; Liu, X.; Mydland, B.L.; Wiswall, J. Systems and Methods for Purifying Aluminum. U.S. Patent 11,001,931, 11 May 2021.
14. Kieft, R.; Bergstrøm, T.; Le Brun, P.; Friedrich, B.; Oygard, A.; Pisch, A.; Rombach, G.; Ryckeboer, M.; Schutter, D.; Sillekens, W. Aluminium Purification. In Proceedings of the ASEM Workshop on Clean Technologies, Hanoi, Vietnam, 3–4 November 2004.
15. Curtolo, D.C.; Rodriguez-Rojas, M.J.; Friedrich, S.; Friedrich, B. Alternative fractional crystallization-based methods to produce high-purity aluminum. *J. Mater. Res. Technol.* **2021**, *12*, 796–806. [CrossRef]
16. Van den Eynde, S.; Bracquené, E.; Diaz-Romero, D.; Zaplana, I.; Engelen, B.; Duflou, J.R.; Peeters, J.R. Forecasting global aluminium flows to demonstrate the need for improved sorting and recycling methods. *Waste Manag.* **2022**, *137*, 231–240. [CrossRef] [PubMed]
17. *UNE-EN 573-3:2020+A1:2023*; Aluminio y aleaciones de aluminio. Composición química y forma de los productos de forja. Parte 3: Composición química y forma de los productos. AENOR: Madrid, Spain, 2023. Available online: https://www.une.org/encuentra-tu-norma/busca-tu-norma/norma?c=N0070803 (accessed on 8 February 2023).
18. Hatch, J.E. *Aluminum Properties and Physical Metallurgy*; American Society for Metals: Metals Park, OH, USA, 1984.
19. Mondolfo, L.F. *Aluminum Alloys*; Butterworth & Co., Ltd.: London, UK, 1976.
20. Davis, J.; Henry, S.; Frueh, S.; Boring, R.; Levicki, D.; Harrision, L.; Scott, W.J. *Aluminum and Aluminum Alloys*; ASM International: Novelty, OH, USA, 1993.
21. Bjurenstedt, A.; Seifeddine, S.; Jarfors, A. The Effects of Fe-Particles on the Tensile Properties of Al-Si-Cu Alloys. *Metals* **2016**, *6*, 314. [CrossRef]
22. Bell, S.; Davis, B.; Javaid, A.; Essadiqi, E. *Final Report on Effect of Impurities in Aluminum*; Natural Resources Canada: Ottawa, ON, Canada, 2006.
23. Altenpohl, D. *Aluminum Viewed from Within*; Aluminium-Verlag: Düsseldorf, Germany, 1982.
24. Humphreys, F.; Hatherly, M. *Recrystallization and Related Annealing Phenomena*; Elsevier Science Ltd.: New York, NY, USA, 1995.
25. Figueiredo, R.; Kawasaki, M.; Langdom, T. Seventy years of Hall-Petch, ninety years of superplasticity and a generalized approach to the effect of grain size on flow stress. *Prog. Mater. Sci.* **2023**, *137*, 101131. [CrossRef]
26. The Aluminum Association. *International Alloy Designations and Chemical Composition Limits for Wrought Aluminum and Wrought Aluminum Alloys*; The Aluminum Association Inc.: Arlington, VA, USA, 2009.
27. Alcan International Limited. *Metallurgy of Al-Mg-Si Alloys*; Alcan International Limited: Banbury, UK, 1972.
28. Poznak, A.; Thole, V.; Sanders, P. The Natural Aging Effect on Hardenability in Al-Mg-Si: A Complex Interaction between Composition and Heat Treatment Parameters. *Metals* **2018**, *8*, 309. [CrossRef]
29. *UNE-EN ISO 6892-1:2020*; Materiales metálicos. Ensayo de Tracción. Parte 1: Método de Ensayo a Temperatura Ambiente. AENOR: Madrid, Spain, 2020.
30. *UNE-EN 515:2017*; Aluminio y Aleaciones de Aluminio. Productos Forjados. Designación de los Estados de Tratamiento. AENOR: Madrid, Spain, 2017.
31. Morris, L.R.; Irichbar, R.; Embury, J.D.; Duncan, J.L. Formability of Aluminum Sheet Alloys. In *Aluminum Transformation Technology and Applications*; American Society for Metals: Metals Park, OH, USA, 1982; pp. 549–582.
32. Lee, B.; Kim, S.; Park, J.; Kim, H.; Lee, J. Role of Mg in simultaneously improving the strength and ductility of Al-Mg alloys. *Mater. Sci. Eng. A* **2016**, *657*, 115–122. [CrossRef]
33. Zupanič, F.; Steinacher, M.; Žist, S.; Bončina, T. Microstructure and Properties of a Novel Al-Mg-Si Alloy AA 6086. *Metals* **2021**, *11*, 368. [CrossRef]
34. Meija, J.; Coplen, T.B.; Berglund, M.; Brand, W.A.; De Bièvre, P.; Gröning, M.; Holden, N.E.; Irrgeher, J.; Loss, R.D.; Walczyk, T.; et al. Atomic weights of the elements 2013 (IUPAC Technical Report). *Pure Appl. Chem.* **2016**, *88*, 265–291. [CrossRef]

35. Santora, E.; Berneder, J.; Simetsberger, F.; Doberer, M. Mechanical properties evolution for 8xxx foil stock materials by alloy optimization-literature review and experimental research. In *Light Metals*; The Minerals, Metals & Materials Series; Springer International Publishing: Berlin/Heidelberg, Germany, 2019. [CrossRef]
36. Zolotorevsky, N.Y.; Solonin, A.N.; Churyumov, A.Y.; Zolotorevsky, V.S. Study of work hardening of quenched and naturally aged Al-Mg and Al-Cu alloys. *Mater. Sci. Eng. A* **2009**, *502*, 111–117. [CrossRef]